ELSEVIER

International Journal of Pharmaceutics 245 (2002) 179–189

international journal of pharmaceutics

www.elsevier.com/locate/ijpharm

In vitro and in vivo dose delivery characteristics of large porous particles for inhalation

Craig Dunbar [a,*], Gerhard Scheuch [b], Knut Sommerer [b], Mark DeLong [a], Alka Verma [c], Rick Batycky [a]

[a] *Alkermes, Inc., 840 Memorial Drive, Cambridge, MA 02139, USA*
[b] *InAMed GmbH, Robert Koch Allee 6, 82131 Gauting, Germany*
[c] *Alkermes Europe Ltd., The Quorum, Barnwell Road, Cambridge CB5 8RE, UK*

Received 21 December 2001; received in revised form 9 April 2002; accepted 1 July 2002

Abstract

The purpose of this study was to evaluate the in vitro and in vivo dose delivery characteristics of two large porous particle placebo formulations with different mass median aerodynamic diameters (MMAD approximately equal to 3 and 5 μm). In vitro dose delivery characteristics were measured using the multistage liquid impinger (MSLI). In vitro lung deposition was predicted by calculating the extrathoracic deposition using the ICRP model, with the remaining fraction assumed to deposit in the lungs. Healthy subjects were trained to inhale through the AIR^{TM} delivery system at a target peak inspiratory flow rate (PIFR) of 60 l/min, The in vivo dose delivery of large porous particles were obtained by γ-scintigraphy and was characterized by high ($\sim$90%), reproducible emitted doses for both the small and large MMAD powders. The mean in vivo lung deposition relative to the total metered dose were 59.0 and 37.3% for 3 and 5 μm MMAD powders, respectively. The AIR^{TM} delivery system produced high in vivo lung deposition and low intersubject CVs (approximately 14%) across the range of PIFRs obtained in the study (50–80 l/min), This is relative to a variety of dry powder inhalers (DPI) that have been published in the literature, with in vivo lung deposition ranging from 13 to 35% with intersubject CVs ranging from 17 to 50%. The ICRP model provided a good estimate of the mean in vivo lung deposition for both powders. Intersubject variability was not captured by the ICRP model due to intersubject differences in the morphology and physiology of the oropharyngeal region. The ICRP model was used to predict the regional lung deposition, although these predictions were only considered speculative in the absence of experimental validation. © 2002 Elsevier Science B.V. All rights reserved.

Keywords: Large porous particles; Lung deposition; Inhalation

1. Introduction

The principal mechanisms contributing to lung deposition are inertial impaction, sedimentation and diffusion (Heyder et al., 1986), The aerosol

* Corresponding author. Tel.: +1-617-250-1532; fax: +1-617-495-0075
E-mail address: craig.dunbar@alkermes.com (C. Dunbar).

0378-5173/02/$ - see front matter © 2002 Elsevier Science B.V. All rights reserved.
PII: S0378-5173(02)00349-6

formulation parameter influencing inertial impaction and sedimentation is the aerodynamic diameter (d_a), with the geometric diameter (d_g) influencing diffusion. Deposition is primarily driven by aerodynamic diameter as diffusion only impacts a small fraction of the dose with small geometric diameters ($d_g < 1.0$ μm). Evaluation of the in vitro dose delivery characteristics from a dry powder inhaler (DPI), therefore, requires an accurate measure of the aerodynamic particle size distribution (PSD) and the dose emitted from the DPI.

Multistage cascade impaction is widely used for the characterization of the aerodynamic PSD. The method is described in the United States and European Pharmacopoeias and is the Food and Drug Administration's method of choice for the release and stability testing of inhaled drug products (EP, 1991; USP, 1999a). The popularity of multistage cascade impaction is due to the instrument's ability to measure the entire mass distribution emitted from the inhaler and the provision of a detailed fractionation of the aerosol drug mass.

There has been poor agreement between the in vitro lung deposition estimated from the aerodynamic PSDs obtained with multistage cascade impaction and in vivo lung deposition data obtained from a variety of inhalation drug delivery systems (Newman et al., 2000). A number of potential causes for this disparity have been investigated. The geometry of the induction port does not reflect that of the oropharynx (Niven et al., 1994; Swift, 1994; Cheng et al., 1999). The non-respirable, high velocity droplets generated by pressurized metered dose inhalers (ballistic component) distorts the aerodynamic PSD (Thiel, 1998). The flow profile used in the cascade impactor may not be representative of the clinical inspiratory flow profile (Clark and Bailey, 1996; Lee et al., 1996; Burnell et al., 1998; Finlay and Gehmlich, 2000). Calibrated flow rates of the cascade impactor may not be representative of the clinical inspiratory flow rates (Nichols and Smurthwaite, 1998). Impactor errors such as bounce, overload, re-entrainment and interstage losses distort the aerodynamic PSD (May, 1945; Rao and Whitby, 1978a,b). The cascade impactor only measures a small particle fraction of the PSD, with large particle fractions depositing in the induction port and preseparator, making it difficult to accurately size the distribution (Dunbar and Hickey, 1999). Furthermore, measurement by inertial impaction of low mass density particles may be influenced by ultra-Stokesian drag and interception effects, i.e. the impactors effective cut-off diameters may not be independent of particle mass density and geometric diameter (Radar and Marple, 1985). Empirical and mathematical models have been developed to predict lung deposition of continuous aerosols (Heyder and Rudolf, 1984; ICRP, 1994). However, bolus aerosol deposition mechanisms are different from those for continuous aerosols and may not be captured by lung deposition models of continuous aerosols (Scheuch and Stahlhofen, 1987). Despite these potential limitations, agreement between in vitro and in vivo lung deposition data is emerging for specific bolus delivery systems (Farr et al., 2000; Price, 2000).

Large porous particles for inhalation are characterized by large geometric diameters (> 5 μm) and low mass densities (< 0.4 g/cc), yielding aerodynamic diameters of approximately 1–5 μm for optimal lung deposition (Edwards et al., 1997). Increasing the geometric diameter increases the dispersibility of the powder, making it possible to efficiently deliver a wide range of doses using a simple, passive DPI. The purpose of this study was to evaluate the in vitro and in vivo dose delivery characteristics of two large porous particle placebo formulations with different aerodynamic PSDs (3 and 5 μm MMAD powders).

2. Methods

2.1. Powders

Two placebo powders were evaluated with different aerodynamic PSDs. One placebo powder had an MMAD approximately equal to 3 μm, the other placebo powder had an MMAD approximately equal to 5 μm as determined by multistage liquid impinger (MSLI) (described in Section 2.4). Both placebos were prepared with the same generally regarded as safe (GRAS) excipients and

excipients endogenous to the lungs using a spray drying process (Vanbever et al., 1999). The PSD characteristics, summarized in terms of the MMAD, volume median geometric diameter (VMGD) and geometric standard deviation (GSD), are shown in Table 1, along with the tap density (ρ_{tap}) of each powder. The VMGD was measured using laser diffraction with an inhaler attachment operated at 60 l/min for a 2 l volume (HELOS, Sympatec Inc., Princcton, NJ). Tap density was measured following USP < 616 > with a mass of 50 mg (USP, 1999b).

2.2. Dry powder inhaler

A passive, capsule based DPI, illustrated in Fig. 1, was used in the study. The inhaler consists of a mouthpiece, dispersion chamber and puncturing mechanism. The mouthpiece is removed and a size two HPMC capsule is placed into the dispersion chamber. The mouthpiece is then attached and the button at the base of the inhaler is depressed to push the staple into the bottom of the capsule, forming two small holes. The subject places the inhaler in their mouth and inhales. The capsule spins due to the motion of the air flowing through the dispersion chamber and the powder is emitted from the inhaler via the mouthpiece.

2.3. Radiolabeling process

The radiolabeling process is shown schematically in Fig. 2. NaCl particles (tagged with ^{99m}Tc) were generated from a Pari LC Star nebulizer (Pari, Starnberg, Germany) containing ^{99m}Tc saline solution (0.5 ml ^{99m}Tc in isotonic saline diluted with 100 ml of deionized water). The droplets were dried in a 100 l drying chamber to form NaCl nanoparticles (estimated from the solute concentration) that were neutralized using a krypton neutralizer (Kr-85, 10 mCi, TS1, St. Paul, MN). The NaCl nanoparticles were distributed through

Table 1
PSD characteristics and tap density (ρ_{tap}) (S.D. shown, $n = 3$)

	3 μm MMAD	5 μm MMAD
MMAD/μm	2.9 (0.1)	5.0 (0.7)
GSD	2.4 (0.2)	1.9 (0.1)
VMGD/μm	7.4 (0.7)	9.9 (0.3)
GSD	2.1 (0.1)	1.9 (0.1)
ρ_{tap}/g/cc	0.06 (0.01)	0.07 (0.01)

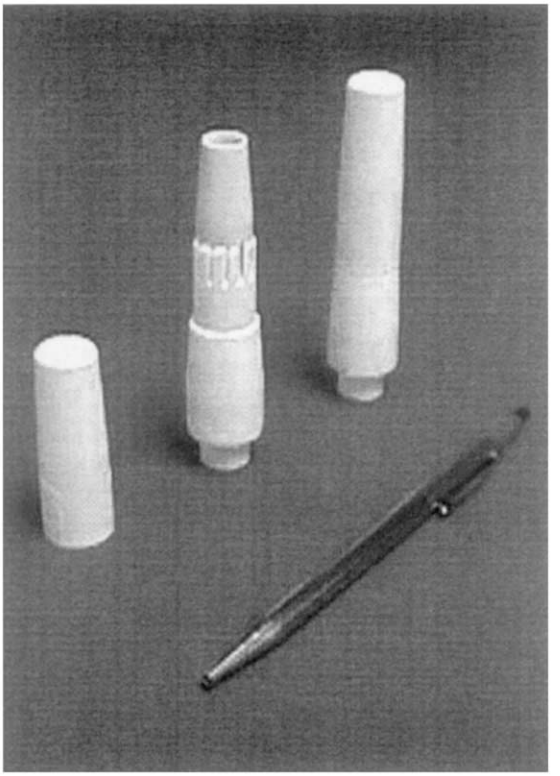

Fig. 1. Dry powder inhaler.

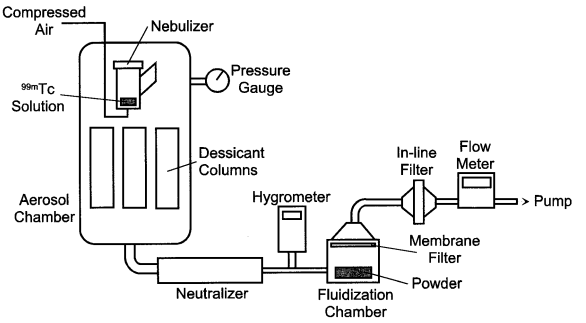

Fig. 2. Schematic of radiolabeling process.

the powder sample using a fluidized bed operated at a flow rate of approximately 7 l/min.

2.4. Radiolabel validation

The emitted dose and distribution of ^{99m}Tc as a function of aerodynamic particle diameter were compared with the mass distribution using a MSLI (Erweka USA, Inc., Milford, CT) with a USP induction port (USP, 1999a). The MSLI was operated at 60 l/min for a total air volume of 2 l. This measurement was performed in triplicate. Powders for validation contained 0.1% by weight rhodamine B, which was added to the solvent system before spray drying. The mass deposited on each stage was analyzed by fluorescence spectrophotometry ($\lambda_{ex} = 547$ nm, $\lambda_{em} = 567$ nm) (F4500, Hitatchi Instruments, San Jose, CA). Mass distributions were obtained for the unlabeled and labeled powder. The ^{99m}Tc deposited on each stage was analyzed by γ-scintigraphy using a high sensitivity Nal detector (Model 905, Perkin–Elmer, Oak Ridge, TN). The MMAD and GSD of the dose emitted from the inhaler were calculated by interpolation from the cumulative fraction undersize. Recoveries were calculated by mass balance using fluorescence spectrophotometry and by activity balance using γ-scintigraphy. In vitro lung deposition of the total dose was calculated across the different powder processes and analytical methods (see Section 2.7).

2.5. Study design

The study was a double blind, randomized, crossover comparison of two inhaled placebo powder formulations, labeled with ^{99m}Tc, 2 days apart, in ten normal female subjects (median age 34.2 years; 21.9–50 years range). 5 ($\pm$1) mg of powder was premetered into a size two capsule and was delivered using the DPI described in Section 2.2. Subjects were trained to attain a PIFR of approximately 60 l/min ($\Delta P = 2.9$ kPa) using a spirometer with an inhaler attachment (PC-Flow+, Spirometrics, Gray, ME). Peak inspiratory flow rate (PIFR) and inhaled volume (V) were measured using the spirometer during the inhaled dose. A breath-hold of approximately 5 s was performed after each inhaled dose. The in vivo emitted dose was determined by measuring the radioactivity in the inhaler pre and post-dose. In vivo lung deposition was determined by γ-scintigraphy using a planar gamma camera (DIACAM, Siemens Gammsonics, Inc., Hoffman Estates, IL) and was defined as the fraction deposited downstream of the trachea (generation 0) relative to the total dose metered into the capsule. Scintigraphic images were obtained immediately after the breath-holding period. Regional deposition in the lungs and stomach were corrected using attenuation factors estimated from the subjects body mass index: (BMI–see Appendix A). Extrathoracic deposition was calculated by subtracting the attenuated lung activity and the activity retained in inhaler, from the total initial activity in the capsule. Subjects were admitted to the study at the time they provided informed consent. Lung function was assessed before and after each inhaled dose.

2.6. Ethics approval

The study was conducted as a modification to an existing project (Nr 201/98; Untersuchung der Deposion und Retention von porosen Aerosolteilchen in der Lunge) being undertaken at the laboratories of InAMed GmbH and Forschungszentrum fur Umwelt und Gesundheit GmbH, Institut für Inhalationsbiologie (GSF), Gauting, Germany. Study approval was obtained from the Ethics Committee of the LMU München and radiation approval obtained from Bayerisches Landeamt für Umweltschutz (LfU, Augsburg, Germany).

2.7. In vitro lung deposition

In vitro lung deposition was predicted by calculating the extrathoracic deposition using the International Commission on Radiological Protection (ICRP) model, with the remaining fraction assumed to deposit in the lungs (ICRP, 1994). Application of the ICRP model was based on the hypothesis that the predicted exhaled fraction for a continuous aerosol would consist of particles that were too small to deposit in the extrathoracic

region and have insufficient time to deposit in the lungs. Therefore, for a passively activated bolus, (a) the same extrathoracic deposition would be obtained as with a continuous aerosol and (b) the particles that would be exhaled for a continuous aerosol would have sufficient time to deposit in the lungs.

In vitro lung deposition of the total dose was calculated for each subject by entering into the model the emitted dose and aerodynamic PSD for a given powder, and entering the sex, height, PIFR and inhaled volume (V), for each individual subject. Deposition of the polydisperse PSD was estimated by fractionating the aerodynamic PSD emitted from the inhaler into segments defined by each stage of the MSLI. In vitro deposition in the trachea was estimated by fractionating the bronchial (BB) deposition by generation volume. This was necessary for comparison with the in vivo lung deposition, that was defined as the fraction of the total dose deposited downstream of the trachea. Inter subject variability in the in vitro lung deposition (expressed as a standard deviation (S.D.) of the mean) was calculated across the subject population.

2.8. Statistical analysis

Pairwise comparison of means was performed using a pairwise t-test. Multiple comparison of means was performed using the Tukey–Kramer method. Comparison of means were tested at $\alpha = 0.05$.

3. Results

Comparison of the in vitro dose delivery characteristics for labeling validation are summarized in Table 2 and Fig. 3. There were no statistically significant differences in the in vitro dose delivery characteristics for the 5 μm MMAD powder across the different powder processes and analytical methods ($P > 0.05$), Small, statistically significant differences were obtained for the 3 μm MMAD powder in terms of the MMAD, GSD and in vitro lung deposition ($P < 0.05$).

Table 3 summarizes the inspiratory maneuver and in vivo dose delivery characteristics obtained with the two powders. The in vivo emitted dose and lung deposition relative to the total dose for each individual subject are shown in Fig. 4. Regional deposition in the lungs and stomach was corrected using attenuation factors calculated for each individual subject. The average BMI attenuation factor for the lungs and stomach was 2.11 (0.25) (S.D. shown in parenthesis). Representative scintigraphic images from a single subject are shown in Fig. 5. There were no statistically significant differences in the mean lung function pre and post-dose across the two powders ($P > 0.05$). Also, there were no clinically significant changes in lung function between pre and post-dose for individual subjects.

The in vitro lung deposition as a function of PIFR are compared with the in vivo data obtained by γ-scintigraphy for the 3 and 5 μm MMAD powders (Fig. 6). Inspiratory maneuvers for two subjects (subject 9, 3 μm MMAD powder; subject 10, 5 μm MMAD powder) were not captured during dosing and are not included in the analysis. Table 4 compares the in vitro and in vivo dose delivery characteristics obtained for both powders. There were no statistically significant differences between the in vitro and in vivo emitted doses for both powders ($P > 0.05$). There were no statistically significant differences between the in vitro and in vivo lung deposition obtained with the 3 μm MMAD powder ($P > 0.05$). Statistically significant differences were obtained between the in vitro and in vivo lung deposition for the 5 μm MMAD powder ($P < 0.05$). The correlation between in vitro and in vivo lung deposition is shown in Fig. 7.

4. Discussion

Large porous particles were radiolabeled with ^{99m}Tc using a fluidized bed method. This method did not affect the in vitro dose delivery characteristics for the 5 μm MMAD powder. Small, statistically significant differences in the in vitro dose delivery characteristics were obtained for the 3 μm MMAD powder ($P < 0.05$). For example, a

Table 2
Comparison of in vitro dose delivery characteristics for the 3 and 5 μm MMAD powders (S.D. shown, $n = 3$)

Powder	Analysis	Emitted dose (%)	MMAD (μm)	GSD	Lung deposition (%)[a]	Recovery (%)
3 μm						
Unlabeled	Fluorescence	90.9 (0.3)	2.9 (0.1)	2.4 (0.2)	60.0 (2.1)	107.0 (7.0)
Labeled	Fluorescence	93.9 (1.5)	3.1 (0.1)	2.5 (0.02)	56.8 (2.2)	94.2 (1.1)
Labeled	Radioactivity	86.3 (10.1)	2.8 (0.1)	2.2 (0.1)	60.0 (2.2)	88.5 (0.2)
5 μm MMAD						
Unlabeled	Fluoresence	91.9 (2.6)	5.0 (0.7)	1.9 (0.1)	45.8 (3.3)	95.6 (1.1)
Labeled	Fluoresence	90.6 (0.8)	4.9 (0.4)	2.0 (0.05)	44.9 (3.0)	96.6 (7.9)
Labeled	Radioactivity	90.0 (1.7)	4.9 (0.2)	2.0 (0.03)	45.1 (3.3)	84.1 (3.7)

[a] $n = 9$.

Table 3
Inspiratory maneuver and in vitro dose delivery characteristics (S.D. shown, $n = 10$)

	3 μm MMAD	5 μm MMAD
PIFR (l/min)[a]	66.5 (10.4)	61.9 (11.4)
Inhaled volume (l)[a]	2.1 (0.4)	2.1 (0.5)
Breath-hold (s)	4.8 (0.8)	5.1 (0.9)
Emitted dose (%)	87.7 (5.0)	87.4 (4.9)
Lung deposition (%)	59.0 (7.7)	37.3 (5.3)
Inhaler (%)	6.4 (4.9)	6.4 (4.0)
Capsule (%)	5.9 (1.3)	6.2 (1.6)
Exhaled air (%)	0.0 (0.0)	0.0 (0.0)

[a] $n = 9$.

small (3.8%), statistically significant difference in the in vitro lung deposition was obtained for the labeled powder with fluorescence analysis relative to the unlabeled powder (fluorescence analysis) and labeled powder (radioactive analysis) ($P < 0.05$). However, there were no statistically significant differences in the in vitro dose delivery characteristics obtained for the 3 μm MMAD unlabeled powder (fluorescence analysis) and labeled powder (radioactive analysis) ($P < 0.05$).

The in vivo dose delivery of large porous particles was characterized by high emitted doses (approximately 90%) with low variability (coefficient of variation (CV) = 6% for both powders) and high lung deposition (59.0% for the 3 μm MMAD powder and 37.3% for the 5 μm MMAD powder) across the range of PIFRs obtained in the study (50–80 l/min), The inter subject lung deposition CVs were 13.0 and 14.2% for the 3 and 5 μm MMAD powders, respectively, showing that the high in vivo lung deposition was reproducible across the range of PIFRs obtained in the study (50–80 l/min). Low inhaler losses were obtained,

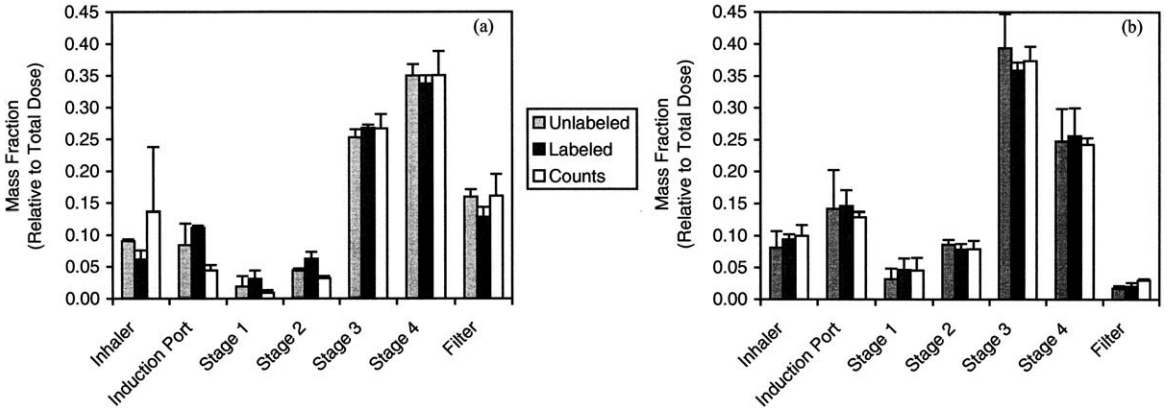

Fig. 3. Comparison of aerodynamic PSDs obtained for (a) 3 μm MMAD powder and (b) 5 μm MMAD powder (S.D. shown, $n = 3$).

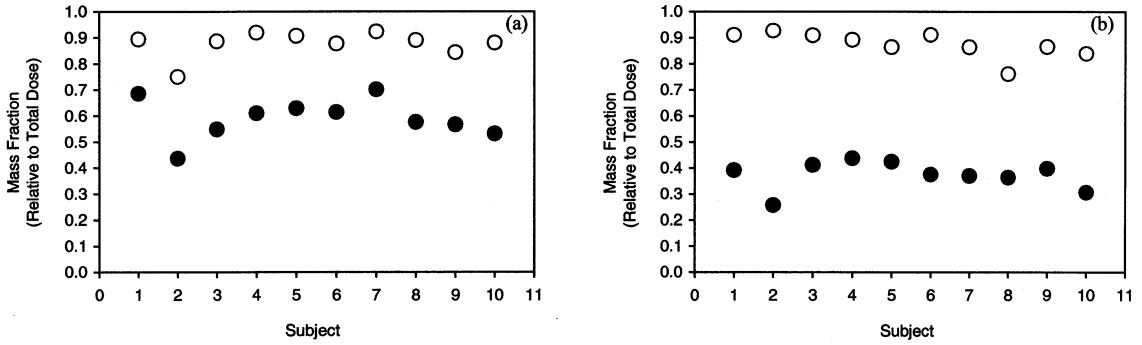

Fig. 4. In vivo emitted dose (○) and lung deposition relative to the total dose (●) for individual subjects, (a) 3 μm MMAD powder and (b) 5 μm MMAD powder.

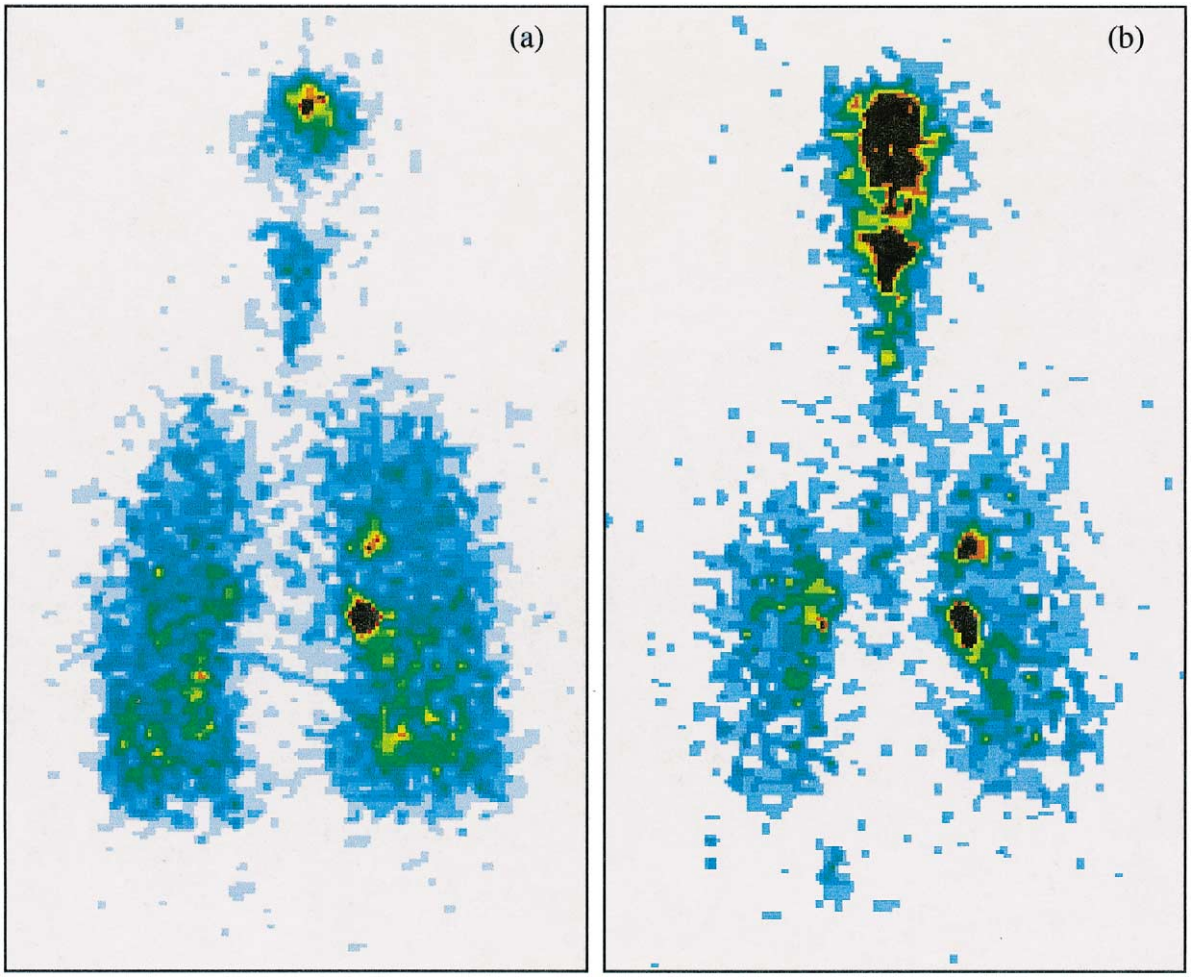

Fig. 5. In vivo lung deposition image obtained by γ-scintigraphy for Subject 1. (a) 3 μm MMAD powder, (b) 5 μm MMAD powder.

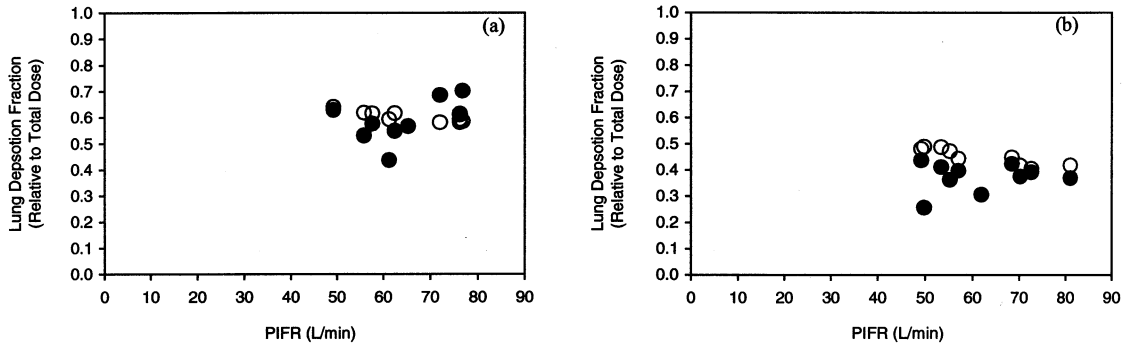

Fig. 6. Lung deposition as a fraction of the total dose obtained in vivo by γ-scintigraphy (●) and in vitro by ICRP model (○) as a function of PIFR for the (a) 3 μm MMAD powder and (b) 5 μm MMAD powder.

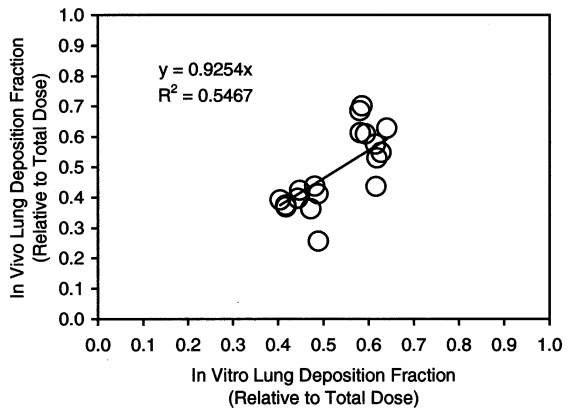

Fig. 7. Correlation between in vivo and in vitro lung deposition fraction relative to the total dose.

with approximately 6% of the total dose being retained in the inhaler. The in vivo lung deposition and intersubject variability of the AIR™ delivery system compared favorably against other passive DPIs. In vivo lung deposition of the total dose from a variety of both passive and active DPIs ranged from 13 to 35%, with intersubject CVs ranging from 17 to 50% (Pitcairn et al., 2000).

The in vitro emitted dose accurately predicted the mean emitted dose obtained in vivo. In vitro lung deposition provided a good estimate of the mean in vivo deposition for both powders. The aerodynamic PSDs were obtained using an MSLI with a USP induction port. The MSLI was selected to accurately characterize the aerodynamic PSD by minimizing the impaction artifacts that occur with solid impaction surfaces, i.e. bounce and overload (May, 1945; Rao and Whitby, 1978a,b). Also, a large fraction of the emitted dose was deposited on the impactor stages ($>85\%$), increasing the accuracy of the aerodynamic PSD measurement (Dunbar and Hickey, 1999). The mass fractions obtained in the MSLI and used in the ICRP model were calculated relative to the emitted dose, i.e. all components downstream of the inhaler, including the induction port, were used to calculate the aerodynamic PSD. Calculation of the aerodynamic PSD based on the mass fractions relative to the mass collected in the impactor

Table 4
Comparison of in vitro and in vivo dose delivery characteristics (S.D. shown, $n = 10$)

	3 μm MMAD		5 μm MMAD	
	Emitted dose (%)	Lung deposition (%)	Emitted dose (%)	Lung deposition (%)
In vitro	86.3 (10.1)[a]	60.6 (2.2)[b]	90.0 (1.6)[a]	45.1 (3.3)[b]
In vivo	87.7 (5.0)	59.0 (7.7)	87.4 (4.9)	37.3 (5.3)

[a] $n = 3$.
[b] $n = 9$.

resulted in an underestimation of the aerodynamic diameter and an overestimation of the predicted lung deposition. For example, the in vitro lung deposition for the 5 μm MMAD powder using the aerodynamic PSD without the induction port was 52.8% compared with 45.1% with the induction port (and 37.3% in vivo).

The ICRP model did not capture the inter-subject variability, as shown by the in vitro–in vivo correlation in Fig. 7 ($R^2 = 0.55$). The in vitro extrathoradc deposition efficiency and the 95% confidence intervals are shown in Fig. 8, along with the in vivo data obtained in the present study. The wide confidence intervals represent the large intersubjcct variability inherent with extrathoracic deposition. This variability is due to intersubject differences in the morphology and physiology of the oropharyngeal region that is not captured by the ICRP model (ICRP, 1994).

The ICRP model was used to predict the in vitro regional deposition, which is beyond the resolution of the planar image generated by γ-scintigraphy. Application of the ICRP model for a bolus aerosol was based on the hypothesis that the model could accurately predict bolus deposition in the extra-thoracic region, with the remaining dose being distributed through the lungs, i.e. the exhaled fractions predicted by the ICRP model were weight-distributed throughout the lungs. For example, the bolus deposition in the bronchial region (BB_{bolus}) was estimated as follows:

$$BB_{bolus} = BB + \frac{BB}{BB + bb + AI} Ex \quad (1)$$

where, Ex represents the exhaled fraction, BB represents the bronchial region, that includes the trachea (generation 0) down to the eighth generation; bb the bronchiolar region, that includes generations 9–15; and AI the alveolar–interstitium region. Fig. 9 shows the predicted in vitro regional deposition obtained from the ICRP model. The difference between the in vitro deposition of the 3 and 5 μm MMAD powders was apparent in the extrathoratic and alveolar regions, with the deposition in the conducting airways (bronchial and bronchiolar) remaining relatively constant. It was recognized that this prediction only provided a speculative estimate of the regional lung deposition. The ICRP model was developed for continuous aerosols and may not be predictive for the regional deposition of bolus aerosols (Scheuch and Stahlhofen, 1987). Significant differences have been shown in the predicted regional deposition obtained from different models, even when good agreement with total lung deposition was obtained (Finlay et al., 2000). This highlights the need to validate in vitro lung deposition models with experimental data that can discriminate between the different morphological regions.

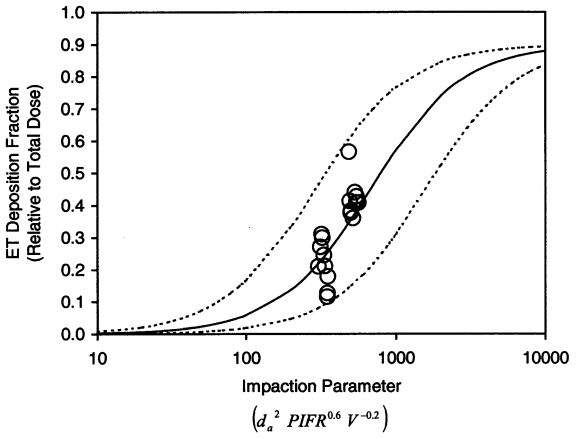

Fig. 8. Comparison of in vitro and in vivo extrathoracic deposition (including 95% confidence limits) relative to the total dose.

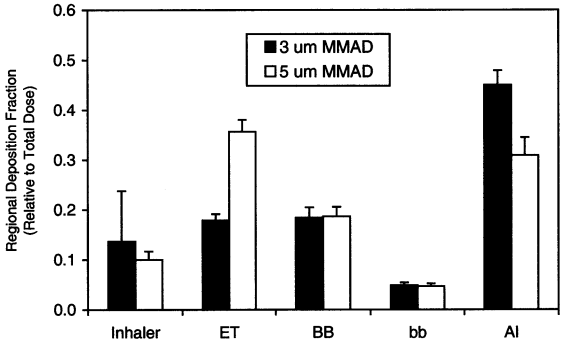

Fig. 9. In vivo regional deposition as a fraction of the total dose (ET = extrathroacic, BB = bronchial; bb = bronchiolar; AI = alveolar-interstitium) (S.D. shown, $n = 9$).

5. Conclusions

The in vivo dose delivery of large porous particles was characterized by high ($\sim$90%), reproducible emitted doses for both the small and large MMAD powders. The mean in vivo lung deposition relative to the total dose were 59.0 and 37.3% for the 3 and 5 μm MMAD powders, respectively. The AIR^{TM} delivery system produced high in vivo lung deposition and low intersubject CVs (approximately 14%) across the range of PIFRs obtained in the study (50–80 l/min). This is relative to a variety of DPIs that have been published in the literature, with in vivo lung deposition ranging from 13 to 35% with intersubject CVs ranging from 17 to 50%. The ICRP model using the aerodynamic PSD measured by the MSLI provided a good estimate of the mean in vivo lung deposition for both powders. Intersubject variability was not captured by the ICRP model due to intersubject differences in the morphology and physiology of the oropharyngeal region. The ICRP model was used to predict the regional lung deposition, although these predictions where only considered speculative in the absence of experimental validation.

Appendix A

Lung deposition attenuation factors were determined using an activity balance method. The inhaled radioactivity was known by measuring the activity injected into a balloon with a high sensitivity γ counter and a γ camera. After the inhalation of the radioactivity from the balloon ($d_a = 2$ μm particles) with a slow inspiratory flow rate, the activity in the lungs of subjects was measured with a γ camera. The radioactivity left in the balloon was also measured again. The attenuation factor was determined from the known inhaled activity and the radioactivity found in the lungs of the subjects. No activity was found in the extrathoracic region. A good correlation between the BMI = Weight/Height^2 and attenuation factor in the lungs was found.

References

Burnell, P., Malton, A., Reavill, K., Ball, M., 1998. Design, validation and initial testing of the electronic lung device. J. Aerosol Sci. 29, 1011–1025.

Cheng, Y.-S., Zhon, Y., Chen, B., 1999. Particle deposition in a cast of human oral airways. Aerosol Sci. Technol. 31, 286–300.

Clark, A., Bailey, R., 1996. Inspiratory flow profiles in disease and their effects on the delivery characteristics of dry powder inhalers. In: Byron, P., Dalby, R., Farr, S. (Eds.), RDD V. Interpharm Press, Inc, Buffalo Grove, IL, pp. 221–230.

Dunbar, C., Hickey, A., 1999. Evaluation of probability density functions to estimate particle size distributions of pharmaceutical aerosols. J. Aerosol Sci. 31, 813–831.

Edwards, D., Hanes, J., Caponetti, G., Hrkach, J., Ben-Jebria, A., Eskew, M., Mintzes, J., Deaver, D., Lotan, N., Langer, R., 1997. Large porous particles for pulmonary drug delivery. Science 276, 1868–1871.

EP 1997. Preparations for inhalation: aerodynamic assessment of fine particles. In European Pharmacopoeia, vol. 5.9.1, European Pharmacopoeia Convention, pp. 143–150.

Fan, S., Warren, S., Lloyd, P., Gkikawa, J., Schuster, J., Rowe, A., Rubsamen, R., Taylor, G., 2000. Comparison of in vitro and in vivo efficiencies of a novel unit-dose liquid aerosol generator and a pressurized metered dose inhaler. Int. J. Pharm. 198, 63–70.

Finlay, W.H., Gehmlich, M.G., 2000. Inertial sizing of aerosol inhaled from two dry powder inhalers with realistic breath patterns versus constant flow rates. Int. J. Pharm. 210, 83–95.

Finlay, W., Lange, C., Li, W.-I., Hoskinson, M., 2000. Validating deposition models in disease: what is needed. J. Aerosol Med. 13, 381–385.

Heyder, J., Rudolf, G., 1984. Mathematical models of particle deposition in the human respiratory tract. J. Aerosol Sci. 15, 697–707.

Heyder, J., Gehhart, J., Rudolf, G., Schiller, C., Stahlhofen, W., 1986. Deposition of particles in the human respiratory tract in the size range 0.005–15 μm. J. Aerosol Sci. 17, 811–825.

ICRP, 1994. Human respiratory tract model for radiological protection. Elsevier Science, Tarrytown.

Lee, K., Suen, K., Yianneskis, M., Marriott, C., 1996. Investigation of the aerodynamic characteristics of inhaler aerosols with an inhalation simulation machine. Int. J. Pharm. 130, 103–113.

May, K.R., 1945. The cascade impactor: an instrument for sampling course aerosols. J. Sci. Instrum. 22, 187–195.

Newman, S., Wilding, I., Hirst, P., 2000. Human lung deposition data: the bridge between in vitro and clinical evaluations for inhaled drug products. Int. J. Pharm. 208, 49–60.

Nichols, S., Smurthwaite, M., 1998. The Andersen cascade impactor: calibration data, operation at various flow rates and modified for use with DPIs at various flow rates. In:

Dalby, R., Byron, P., Farr, S. (Eds.), RDD VI. Interpharm Press, Buffalo Grove IL, pp. 393–396.

Niven, R., Lott, F., Ip, A., Somaratne, K., Kearney, M., 1994. Development and use of an in vitro system to evaluate inhaler devices. Int. J. Pharm. 101, 81–87.

Pitcairn, G., Lankinen, T., Seppala, O.-P., Newman, S., 2000. Pulmonary drug delivery from the Taifun dry powder inhaler is relatively independent of the patient's insptratory effort. J. Aerosol Med. 13, 97–104.

Price, A., 2000. Validation of aerosol deposition models for pharmaceutical purposes: the way forward. In: Dalby, R., Byron, P., Farr, S., Peart, J. (Eds.), RDD VII. Serentec Press, Raleigh, NC, pp. 197–208.

Radar, D., Marple, V., 1985. Effect of ultra-Stokesian drag and particle interception on impaction characteristics. Aerosol Sci. Technol. 4, 141–156.

Rao, A.K., Whitby, K.T., 1978a. Non-ideal collection characteristics of inertial impactors-I. Single stage impactors and solid particles. J. Aerosol Sci. 9, 77–86.

Rao, A.K., Whitby, K.T., 1978b. Non-ideal collection characteristics of inertial impactors-II. Cascade impactors. J. Aerosol Sci. 9, 87–100.

Scheuch, G., Stahlhofen, W., 1987. Particle deposition of inhaled boluses in the upper human airways. J. Aerosol Sci. 18, 725–727.

Swift, D., 1994. The oral airway – a conduit or collector for pharmaceutical aerosols? In: Byron, P., Dalby, R., Farr, S. (Eds.), RDD IV. Interpharm Press, Inc, Buffalo Grove, IL, pp. 187–195.

Thiel, C., 1998. Can in vitro particle size measurements be used to predict pulmonary deposition of aerosol from inhalers. J. Aerosol Med. 11, S43–S52.

USP, 1999a. Aerosols, metered-dose inhalers and dry powder inhalers. In United States Pharmacopoeia, United States Pharmacopelal Convention, Rockville, MD, pp. 4933–4949.

USP, 1999b. Bulk density and tapped density. In United States Pharmacopoeia, United States Pharmacopeial Convention, Rockville, MD, pp. 4950–4951.

Vanbever, R., Mintzes, J., Wang, J., Nice, J., Chen, D., Batycky, R., Langer, R., Edwards, D., 1999. Formulation and characterization of large porous particles for inhalation. Pharm. Res. 16, 1735–1742.